Accepted Manuscript

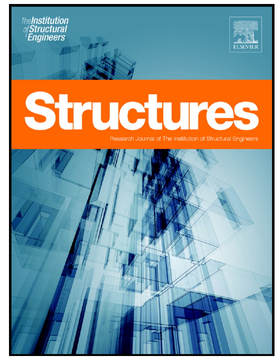


# Fiber Reinforced Polymer as External Reinforcement for Single Cast-in Anchors in Plastic Hinge Zones

Jian Zhao, Derek Petersen, Zhibin Lin, Baolin Wan


| | |
|---|---|
| PII: | S2352-0124(17)30071-1 |
| DOI: | doi:10.1016/j.istruc.2017.11.001 |
| Reference: | ISTRUC 233 |
| To appear in: | *Structures* |
| Received date: | 21 July 2017 |
| Revised date: | 2 October 2017 |
| Accepted date: | 5 November 2017 |

Please cite this article as: Jian Zhao, Derek Petersen, Zhibin Lin, Baolin Wan , Fiber Reinforced Polymer as External Reinforcement for Single Cast-in Anchors in Plastic Hinge Zones. The address for the corresponding author was captured as affiliation for all authors. Please check if appropriate. Istruc(2017), doi:10.1016/j.istruc.2017.11.001

# Fiber Reinforced Polymer as External Reinforcement for Single Cast-in Anchors in Plastic Hinge Zones

Jian Zhao[1*], Derek Petersen[2], Zhibin Lin[3], and Baolin Wan[4]

**ABSTRACT**: This paper presents a test of cast-in anchors in the plastic hinge zone of a reinforced concrete column. Design codes, such as ACI 318-11, do not allow concrete anchors in concrete that could be substantially damaged during an earthquake unless special reinforcement is provided. Steel reinforcement has been proven effective in protecting core concrete; however, it does not protect cover concrete, which is critical to the shear behavior of anchors. Fiber reinforced polymer (FRP) composite material was used in this study to protect cover concrete around the test anchors. The column specimens were subjected to quasi-static cyclic loading while the single anchors were loaded in cyclic shear. Compared with the anchors in unprotected concrete, the FRP reinforced anchors developed a higher shear capacity at a much smaller displacement. This indicates that FRP fabrics can be effective as external reinforcement for concrete anchors. Meanwhile, a systematic study is needed before practical applications.

**Subject headings**: cast-in anchors; carbon fiber; fiber reinforced polymer (FRP); plastic hinge zone; reinforced concrete; and seismic design.

[1] Associate Prof., Dept. of Civil and Environmental Engineering, Univ. of Wisconsin, Milwaukee, WI.
E-mail: jzhao@uwm.edu.
[*]: Corresponding author.
[2] Design Engineer, Koppers Railroad Structures, Madison, WI. E-mail: PetersenDJ@koppers.com
[3] Assistant Prof., Dept. of Civil and Environmental Engineering, North Dakota State University, Fargo, ND.
E-mail: zhibin.lin@ndsu.edu
[4] Associate Prof., Dept. of Civil, Construction and Environmental Eng., Marquette University, Milwaukee, WI.
E-mail: baolin.wan@marquette.edu

## 1. Introduction

Concrete anchors are needed to connect structural steel members to concrete. For example, reinforce concrete frames have been strengthened using steel braces (Badoux and Jirsa 1990), which are fixed to concrete beam/column ends using concrete anchors, as illustrated in Figure 1. The anchor bolts in such connections on the side faces of a concrete frame are subjected to cyclic shear during an earthquake.

The behavior of concrete anchors as a connection between steel members and concrete has been extensively studied, as summarized by Cook and Klingner (1992) and Pallarés and Hajjar (2010). Typical failure modes for such anchors in shear are anchor steel fracture and concrete breakout failure (ACI 318 2011). Anchor steel failure is caused by fracture of the anchor shaft in shear while concrete breakout failure is marked by a concrete cone broken away from the base concrete, in which the connection is located. Anchors with a small edge distance in the shear direction, such as those in the connections in Figure 1, may be controlled by concrete breakout.

Concrete breakout is a brittle failure mode and thus not preferred for connections in seismic zones (Petersen et al. 2013a). Anchor reinforcement, such as V-shaped hairpins encasing the anchor shaft or surface reinforcement, are recommended in ACI 318-11 to transfer shear on an anchor to the bars. Petersen and Zhao (2013) have proposed an alternative design method for anchor shear reinforcement, consisting of closely spaced stirrups, corner bars, and crack-controlling bars. Their tests show that the anchors with the anchor shear reinforcement achieved greater capacities compared with those without reinforcement. Concrete breakout was prevented and anchor shaft fracture was observed in all the tests. However, cover concrete in front of the anchor bolts spalled, as shown in Figure 2. Consequently, the top portion of the anchor shaft under shear loading lost the lateral support from the concrete, causing a combination of shear, bending, and tension in the shaft. An analysis by Lin et al. (2011) indicated that the shear capacity and stiffness of such exposed anchors can be greatly reduced.

Beam/column ends, where anchor connections in Figure 1 are placed, are likely to develop damages during an earthquake (Ibarra and Krawinkler, 2005). It is envisioned that the damage to the concrete cover in plastic hinge zones may adversely impact the cover spalling observed in undamaged/unstressed concrete (Figure 2). One way to protect cover concrete around an anchor in shear is to provide external reinforcement using bonded fiber reinforced polymer (FRP) fabrics.

FRP composite materials have been used extensively to strengthen concrete structures because of their high strength, low density and resistance to corrosion (Bakis et al. 2002; Teng et al. 2002; Wan 2014). Specifically, FRP fabrics have been used to wrap around concrete columns or piers to increase their capacity and ductility (Mirmiran et al. 1998; Moran and Pantelides 2002; Wu et al. 2006; Jiang and Wu 2012). FRP jacketing on the plastic hinge region of reinforced concrete columns has become a common technology to strengthen the seismic resistance capacities.

FRP wrapping has not been used as external reinforcement for concrete anchors. In this paper, a laboratory test is presented to demonstrate the potential of FRP wrapping to protect cover concrete around single anchors installed in the plastic hinge zone of a concrete column.

## 2. Materials and Methods

### 2.1 Reinforced Concrete Column Specimen

A total of six reinforced concrete (RC) columns were used in this study of the single anchors embedded in plastic hinge zones while two shear tests are reported in this paper. The RC columns had a section of 305×305 mm [12×12 in.] and a height about 1.5 m [5 ft.] from the top face of the base block, as shown in Figure 3. The column base block had a dimension of 1219×240 mm [48×20 in] and a height of 432 mm [17 in.]. Two tie-down points were 0.91 m [3 ft.] from the center of the column. The horizontal loads were applied to the top of the column at 1.57 m [62 in.] from the base through a steel loading block.

Eight No. 5 bars (ASTM Grade 60) were provided as the longitudinal reinforcement for the columns. The concrete cover was 38 mm [1.5 in.], typical for RC members with interior exposure (ACI 318 2011). A section analysis with the actual material properties shown below indicated that the column had a nominal moment capacity about 105.8 kN-m [78 k-ft.]. This corresponded to a lateral load capacity about 67.4 kN [15 kips] at the top of the column. A shear design calculation for this ultimate load led to No. 4 ties at a spacing of 152 mm [6 in.], as illustrated in Figure 3. The shear forces from the test anchors were expected to be transferred to foundation block directly.

**2.2 Test Anchors**

The test anchors were made from 19-mm [¾-in.] diameter ASTM A193 Grade B7 threaded rods. The net shear area ($A_{sa,V}$) for the threaded rods was 2.2 cm$^2$ [0.334 in.$^2$]. Each test anchor has a theoretical shear capacity ($V_u$) of 117 kN [26.4 kips] according to ACI 318 (2011). The test anchor had an embedded depth ($h_{ef}$) of 203 mm [8 in.], and located near the middle of the column side faces. With this configuration, one anchor would have a front edge distance of 138 mm [5.4 in.] while the other 167 mm [6.6 in.], as shown in Figure 3. The edge distances for the test anchors switched when the applied shear forces reversed the direction.

The test anchors were placed 203 mm [8 in.] above the base block. The length of the plastic hinge zone was assumed as 0.46 m [18 in.] (that is 1.5 times the column section height), as marked in Figure 3. The anchor position was selected assuming a crack spacing of 51 mm [2 in.]

such that a major flexural crack would likely pass through the test anchors.

### 2.3 FRP External Reinforcement

FRP fabric was used in Specimen S3 to protect the cover concrete. The single-layer FRP fabric (QuakeWrap™ TU27C carbon fabric from QuakeWrap, Inc.) was attached to the column using QuakeBond J300SR saturating resin. The column edges were rounded to a radius of 19 mm [0.75 in.] following the manufacturer's recommendation. According to the datasheet, the FRP fabric has a breaking force of 30 kN [6.8 kips] per inch width. With cover spalling prevented with the FRP wrapping, the test anchors were expected to develop their full shear capacity (117 kN [26.4 kips] each). The required FRP fabric width was calculated as 99 mm [3.9 in.] for this load, and a 51-mm [2-in.] fabric was placed on each side of the test anchors, as shown in Figure 4.

The QuakeWrap product line is developed mainly for structural strengthening. The FRP fabrics were wrapped around the column and overlapped by 305 mm [12 in.] on the north side of the column. This corresponded to an overall development length about 457 mm [18 in.]. According to a study of the bond strength of FRP fabrics mounted at the bottom face of RC beams by Hassan and Rizkalla (2003), the maximum tensile load that can be developed through FRP-concrete bond is 129 kN [28.9 kips]. Debonding, on the other hand, was not expected for the entire FRP fabrics in this study because of the 90-degree bent 152 mm [6 in.] from the anchor, as shown in Figure 4.

### 2.4 Materials

Ready mixed concrete with Wisconsin Department of Transportation Type A-FA mixture was used. The specified concrete compressive strength was 27.6 MPa [4000 psi]. The hardened concrete had a compressive strength of 40 MPa [5800 psi] at 28 days, and the compressive strength went up to 47.6 MPa [6900 psi] at about 84 days, when the tests presented in this paper were conducted.

The No. 5 reinforcing steel bars had a nominal yield strength of 414 MPa [60 ksi]. The measured stress-strain relationship indicates a yield strength of 448 MPa [65 ksi] using the 0.2% offset method. The ultimate strength of the reinforcing bars was measured 696 MPa [101 ksi] at a strain about 0.15. In addition, from the stress-strain relationship of ASTM A193 Grade B7 rods, the yield strength was measured 724 MPa [105 ksi] corresponding to a 0.2 percent plastic strain, and the measured ultimate strength was 914 MPa [132 ksi] at a strain about 0.045.

**2.5 Test Setup and Loading Protocol**

The test setup is shown in Figure 5. The column specimen was fixed to the strong floor of the laboratory using two high-strength threaded rods. An MTS Model 244.31, 245-kN [55-kip] actuator was used to apply a reversed cyclic displacement at the top of the column. Another MTS Model 244.31 actuator was used to apply shear forces to the anchors through a loading adapter. Two single anchors, one installed on each side of the RC column, were loaded simultaneously to eliminate the torsion to the RC column. The centerline of this actuator was located at the height of the test anchors.

Linear potentiometers and linear variable differential transformers (LVDTs) were used to monitor the behavior of the test columns and the anchors. While the instrumentation details can be found elsewhere (Petersen et al. 2013b), a series of strain gages were used to monitor the deformation in the FRP fabrics. Specifically, strain gages installed on the second fiber bundle below the test anchor, as shown in Figure 4. For the east side anchor, a total of seven gages were installed with a center-on-center spacing on 25.4 mm [1 in.]. The west side had only five gages, as limited by the data acquisition system.

The columns were subjected to reversed cyclic displacements. The displacement history included groups of three cycles with the peak displacements corresponding to ±Δy, ±2Δy, ±3Δy, ±4Δy, ±6Δy, and ±8Δy. The yield displacement (Δy) was determined using a fiber-based analysis of the columns. The loading rate for displacement cycles were kept at 6 mm/min [0.24 in./min] throughout the tests.

The anchors in Specimen S1 were loaded in monotonic shear till failure after the column was subjected to the predefined loading history described above. The anchors in Specimen S3 were loaded in reversed cyclic loading simultaneously with the column loading. The anchor loading was in load control, and the peak loads were determined assuming the anchors can develop their full shear capacity, as predicted below: ±27, ±53, ±80, ±107, ±160, and ±214 kN [±6, ±12, ±18, ±24, ±36, and ±48 kips]. The loading on the test anchors was in the same direction as the loads on the column to reflect the loading on the anchor connections in Figure 1.

## 3. Theory and Calculation

The full shear capacity of the concrete anchors, according to ACI 318-11, was calculated from

$$V_u = 0.6 f_{uta} A_{se,V}, \tag{1}$$

where $f_{uta}$ is the ultimate tensile strength of the anchor steel and $A_{se,V}$ is the net shear area of the anchor shaft. Meanwhile, ACI 318-11 stipulates that the design shear strength of anchor bolts with a grout leveling pad shall be reduced by a factor of 0.8. A 3-mm [1/8- in.] gap was maintained in this study between the loading plate and the concrete surface to protect the strain gages. In this case, the shear capacity was calculated based on a model by Lin et al. (2011). Specifically, the shear capacity of anchor bolts with an exposed length (*l*) was calculated as

$$V_{se} = f_{ya} A_{se,v} \sin(\beta) + \frac{f_{ya}\cos(\beta)}{\frac{1}{0.9 A_{se,v}} + \frac{l}{3.4S}}, \tag{2}$$

where $f_{ya}$ is the yield strength of anchor steel, $S$ is the section modulus of the test anchor, and the rotation angle of the exposed anchor ($\beta$) is estimated as $\theta + l_p \tan^{-1}\frac{\varepsilon_{max}}{d_a}$, in which the maximum tensile strain ($\varepsilon_{max}$) was obtained from the anchor material; $\theta$ is the initial end rotation allowed by the oversized holes and/or concrete deformation, $l_p$ is the length of plastic hinge developed in anchor shaft at the ultimate load, and may be taken as $d_a$ (nominal diameter of the anchor) or $l/2$ for anchors with a short exposed length.

The exposed length ($l$) for the anchors in Specimen S1 was expected to be around 51 mm [2 in.] because of the potential cover spalling. The calculated end rotation angle ($\beta$) was about 10 degrees, and the predicted shear capacity for each anchor in Specimen S1 was 60 kN [13.5 kips]. This length ($l$) for the anchors in Specimen S3 was expected to be 4.4 mm [0.17 in.] as the cover concrete was protected by the 1.2-mm [0.05-in.] thick FRP fabrics. Correspondingly, the calculated anchor shear capacity for each anchor in Specimen S3 was 110 kN [24.8 kips], which is slightly smaller than the code-stipulated full capacity as predicted using Eq. 1.

## 4. Results and Discussion

### 4.1 Column Behavior

The column in Specimen S1, loaded before testing the anchors, had a typical hysteretic behavior found in flexural members, as shown by the dashed lines in Figure 6. The unsymmetrical behavior in two loading directions was attributed to a 19-mm [¾-in.] offset of the column at the top. An examination of the strains in the middle longitudinal bar indicated that the first yield occurred during the loading cycle at about 13 mm [0.5 in.]. The largest column displacement was about 102 mm [4 in.], corresponding to $8\Delta_y$ at a peak load about 67 kN [15 kips].

The local FRP wrapping was designed only to protect cover concrete near the test anchors, and thus was not applied to the entire plastic hinge zone of the column specimen as shown in Figs. 4 and 5. Therefore, the behavior of Column S3 was not expected to improve compared with Column S1, as the damage occurred to the concrete in the plastic hinge zone just below the FRP fabric, as shown later in Fig. 8. Meanwhile, the solid lines in Figure 6 indicates that the load-displacement behavior of Column S3 was affected by the simultaneous loading to the anchors. The required loads on the column top at designated displacements were in general smaller because of the large forces on the anchors in the same direction. A data analysis indicates that the lateral loads on the column top, combined with the loads on the test anchors, generated similar sectional behavior to Column S1.

### 4.2 Anchor Behavior in Shear

#### *4.2.1 Behavior of anchors without FRP protection (Specimen S1)*

The behavior of the two single anchors subjected to monotonic shear is shown in dashed lines in Figure 7. The east anchor had a slightly larger shear displacement partly because of a smaller edge distance. The X-axis in Figure 7 thus shows the average shear displacement measured relative to the concrete front face in the load-displacement curve. The Y-axis shows the total shear resistance from the two single anchors. The anchors behaved elastically till about 33.4 kN [7.5 kips], beyond which the slope reduced significantly, indicating the crush of concrete in front of the anchor shafts. Cracks on the east side face first showed up at a load of 89 kN [20 kips] followed by spalling of concrete cover as shown later in Figure 8a.

The shear force increased with a relatively high slope beyond 111.2 kN [25 kips] corresponding to a displacement about 19 mm [0.75 in.]. Similar observation has been made in a previous study (Petersen and Zhao 2013): the anchor shafts bent when the concrete cover spalled, and carried the shear load partially in tension. Therefore, the anchor shear behavior had contributions from anchor shaft in shear, bending, and tension as indicated by Eq. 2. The east anchor fractured while the west anchor was also significantly bent, when the combined load was 175 kN [39.4 kips]. On average, each anchor had a shear capacity of 87.5 kN [19.7 kips], which is larger than the predicted shear capacity shown above. An after-test examination indicated that the test anchors were bent to an angle about 23 degrees instead of the assumed 10 degrees. The predicted shear capacity becomes 92 kN [20.7 kips] when the actual angle in the anchor shaft is used.

The shear capacity of the anchors in Specimen S1 was achieved after the anchors experienced a large deformation of 23 mm [0.9 in.]. This large deformation would adversely impact the behavior of the diagonal braces shown in Figure 1 if the anchors were installed in column ends without proper cover protection. Note that the cover spalling, as shown in Figure 8a, was partially attributed to the damage to the concrete in the plastic hinge zone of the column S1.

*4.2.2 Behavior of anchors with FRP protection (Specimen S3)*

The cover concrete around the anchors in Specimen S3 was protected by FRP fabrics, as shown in Figure 4. Therefore, the behavior of the anchors in Specimen S3 was greatly improved. The load vs displacement behavior of the anchors in Specimen S3 is plotted in Figure 9. Again, the displacement in the plot is the average displacement measured from LVDTs, and the load is the combined shear resistance from two test anchors. The overall load-displacement behavior seems abnormal compared to that of a typical structural element: 1) the loading and reloading branches do not always have a positive slope; 2) the peak displacements do not increase with an increase in the apply peak load; and 3) the unloading braches have positive slopes. The interaction between the two actuators in Specimen S3 is deemed the reason for the observed anchor behavior and the column behavior in Figure 6: the loading rates for both actuators were selected such that the peak loads on the test anchors would be achieved when the peak displacements were applied to the column top; however, this synchronized loading was not always maintained during the loading. Specifically, the column unloading may have been at a faster pace than the anchor unloading; therefore, the anchors experienced decreased deformation at loading stages and increasing deformation during unloading stages.

The cyclic anchor behavior is simplified, as shown by the solid lines in Figure 7, which were created by connecting the first peak point of all five loading groups shown in Figure 9. One point (shown by a cycle) is added corresponding to the apparent yield load ($0.6 f_{yta} A_{s,V}$) of 187 kN [42 kips]. In addition, the last point (shown by a square in Figure 7) is a random point on the unloading path indicated that the fracture occurred during this loading cycle. The anchors in Specimen S3 had a rigid behavior all the way up to the maximum loads. The displacements corresponding to the two peak loads in both directions are about 2.5 mm [0.1 in.] though the displacement measurements may be affected by the column deformation. This rigid behavior is beneficial to the anchor connection and the brace in Figure 1.

Within each loading group, the anchors had an increased displacement during the second and third cycles compared with the first loading cycle. This indicated that the concrete in front of the anchors crushed as shown in Figure 8b, and the crushed concrete did not recover upon unloading. The anchors were able to carry a combined shear of 214 kN [48 kips] in the positive direction, which is very close to the predicted anchor shear capacity shown above. The anchor shaft on the east side fractured at a combined load of -191 kN [-43 kips] when the loading was reversed (Figure 8b). The fracture was mainly attributed to low cycle fatigue.

**4.3 Behavior of FRP fabrics**

Unlike Specimen S1, the concrete cover spalling did not occur to Specimen S3. The FRP fabrics protected the cover concrete near the test anchors as expected. The FRP wrapping also protected column segment from severe damage under lateral loads. Note that the behavior of the RC column did not see any improvement because the damage below the FRP wrapping controlled the behavior of the column, as shown in Figure 8b.

Strain gages were installed on the second fiber bundle below the anchor bolts, as shown in Figure 4. The measured strains, corresponding to the first peak load in each loading group, are summarized in Figure 10. Note that these strain gages placed on the second fiber bundle may not represent the deformation in the entire 51-mm [2-in.] FRP fabrics because the FRP fabrics were unidirectional and the cross links between fiber bundles were deemed weak.

When the applied load on the east anchor was positive, the anchor had a front edge distance of 150 mm [5.4 in.], and the potential cover spalling is illustrated by the curved lines in the inserted picture in Figure 10a. The fiber strain in front of this anchor is the highest, and the fiber strains in general decrease as the gaged location moves away from the anchor. This indicates that the tensile force in this fiber gradually transferred to concrete through FRP-concrete bond when the loads on the test anchors were below their shear capacities. Meanwhile, the fiber strains were largely uniform at about 3000 microstrains from all six gages behind the anchor when the anchor load was at 214 kN [48 kips], indicating that the debonding occurred and the FRP fabrics were developed through the overlap on the north face. A close examination confirmed the debonding near the east anchor, as shown in Figure 8b.

When the applied load on the east anchor was negative, the anchor had a front edge distance of 168 mm [6.6 in.]. The strains from the five gages on the north side were negative as shown in Figure 10b when the applied load was below 107 kN [24 kips], indicating that the concrete was in compression. Beyond this load, the cover spalling may have initiated as all the fiber strains are positive, and comparable to those under the positive load at the same level (e.g., 160 kN [36 kips]). Note that the strain measurements, marked by the dashed lines in Figure 10b, were noisy and likely unreliable under the load of 191 kN [43 kips]. Nevertheless, the maximum fiber strain was about 6500 microstrains at both peak loads. These maximum strains are comparable to the peak strains measured by Hassan and Rizkalla (2003) using a 500-mm [20-in.] long FRP fabric.

Similar observations can be made for the west anchor, as shown in Figures 10c and 10d. When a positive load was applied to the anchors, the west anchor had a front edge distance of 168 mm [6.6 in.]. Correspondingly, the fiber strains were negative when the applied load was small. All fiber strains were positive and roughly same at the peak load of 214 kN [48 kips]. When a negative load was applied to the anchors, the west anchor had a front edge distance of 150 mm [5.4 in.]. Again, at the peak load, all four gages picked up similar readings, indicating that debonding occurred to the FRP fabric near the test anchor.

## 5. Conclusion

Steel braces may be used to strength reinforced concrete (RC) frames, in which anchor connections must be installed in the plastic hinge zones of RC members. The current design codes, such as ACI 318-11, require special reinforcement for anchors in potentially damaged concrete. Anchor reinforcement has been developed for anchors in shear or tension, and verified using tests of single cast-in anchors embedded in undamaged concrete and significantly damaged concrete.  The test results indicate that the special anchor reinforcement can be effective in protecting core concrete; however, the steel reinforcement cannot protect cover concrete, which is critical for the anchor shear behavior.

Fiber reinforced polymer (FRP) wrapping was attempted in this study to protect cover concrete near the anchors installed in the plastic hinge zone of a reinforced concrete column. The FRP fabrics were proportioned to carry the full design shear capacity of the anchors. The column was subjected to reversed cyclic deformation while the test anchors were simultaneously subjected to reversed cyclic loading. Compared with the anchors in unprotected concrete (Specimen S1), the anchors embedded in the concrete protected by two 51-mm [2-in.] wide FRP fabrics (Specimen S3) developed much higher shear capacity, and allowed much smaller deformation. This was largely attributed to the fact that the cover concrete spalled in Specimen S1 while the spalling was restrained by the FRP wrapping.

It is envisioned that a stiff connection is critical for the desired seismic performance of the steel braces. FRP wrapping seems a viable solution in this case. Meanwhile, further study is needed to better understand the effectiveness of FRP wrapping and to determine the anchorage requirements of the FRP fabrics as external reinforcement for concrete anchors.

## 6. Acknowledgments

The study reported in this paper is from a project funded by the National Science Foundation (NSF) under Grant No. 0724097. The project could not complete without contribution from many UWM undergraduate students. The authors gratefully acknowledge the support of Dr. Joy Pauschke, who served as the program director for this grant. Any opinions, findings, and recommendations or conclusions expressed in this paper are those of the authors, and do not necessarily reflect the views of NSF.

**References**


1. American Concrete Institute (ACI) Committee 318, (2011) "Building Code Requirements for Structural Concrete (ACI 318-11)." Farmington Hills, MI.
2. Badoux, M. and Jirsa, J., (1990) "Steel bracing of RC frames for seismic retrofitting," ASCE Journal of Structural Engineering, Vol. 116(1), pp. 55-74.
3. Bakis, C.E., Bank, L.C., Brown, V.L., Cosenza, E., Davalos, J.F., and Lesko, J.J. (2002) "Fiber-Reinforced Polymer Composites for Construction State-Of-The-Art Review", *ASCE Journal of Composite for Construction*, Vol. 6, No. 2, pp 73-87.
4. Cook, R. A., and Klingner, R. E. (1992). ''Ductile multiple-anchor steel to-concrete connections.'' Journal of Structural Engineering, vol. 118 no. 6, pp.1645–1665.
5. Ibarra L. F., and Krawinkler, H. (2005). "Global collapse of frame structures under seismic excitations", Report No. TB 152, The John A. Blume Earthquake Engineering Center, Stanford University, Stanford, CA.
6. Jiang, J. F., and Wu, Y. F. (2012). "Identification of Material Parameters for Drucker-Prager Plasticity Model for FRP Confined Circular Concrete Columns." International Journal of Solids and Structures, 49(3-4), 445-456.
7. Lin, Z., Luke, B., Shahrooz, B., and Zhao, J. (2013) "Headed Anchors in Plastic Hinge Zone of Reinforced Concrete Members." Final Report (Volume III) for Project - Behavior and Design of Cast-in-Place Anchors under Simulated Seismic Loading. University of Wisconsin, Milwaukee, WI.
8. Lin, Z., Petersen, D. Zhao, J., and Tian, Y. (2011) Simulation and design of exposed anchor bolts in shear. *International Journal of Theoretical and Applied Multiscale Mechanics*. vol. 2, pp. 111-119.

9. Mirmiran, A., Shahawy, M., Samaan, M., Echary, H. E., Mastrapa, J. C., and Pico, O. (1998). "Effect of column parameters on FRP confined concrete." *Journal of Composites for Construction*, Vol. 2, No. 4, pp. 175-185.

10. Moran, D.A. and Pantelides, C.P. (2002) “Variable strain ductility ratio for fiber-reinforced polymer-confined concrete”, *Journal of Composites for Construction*, Vol. 6, No. 4, pp 224-232.

11. Pallarés, L. and Hajjar, J. (2010). “Headed steel stud anchors in composite structures, Part I: Shear.” *Journal of Constructional Steel Research*, vol. 66, no. 2, pp.198-212.

12. Petersen, D., Lin, Z., and Zhao, J. (2013a) "Reinforcement for Headed Anchors." Final Report (Volume I) for Project - Behavior and Design of Cast-in-Place Anchors under Simulated Seismic Loading. University of Wisconsin, Milwaukee, WI.

13. Petersen, D., Lin, Z., and Zhao, J. (2013b) "Reinforcement for Headed Anchors." Final Report (Volume II) for Project - Behavior and Design of Cast-in-Place Anchors under Simulated Seismic Loading. University of Wisconsin, Milwaukee, WI.

14. Petersen, D. and Zhao, J. (2013) Design of Anchor Reinforcement for Seismic Shear Loads. *ACI Structural Journal*. Vol. 110, No. 1, pp.53-62.

15. Teng, J.G., Chen, J.F., Smith, S.T., and Lam, L. (2002) *FRP Strengthened RC Structures*, UK: John Wiley and Sons.

16. Wan, B. (2014), “Using fiber-reinforced polymer (FRP) composites in bridge construction and monitoring their performance: an overview”, Chapter 1, *Advanced Composites in Bridge Construction*, Kim, Y.J., Ed., Woodhead Publishing Limited.

17. Wu, G., Lü, Z. T., and Wu, Z. S. (2006). "Strength and ductility of concrete cylinders confined with FRP composites." *Construction and Building Materials*, 20(3), 134-148.

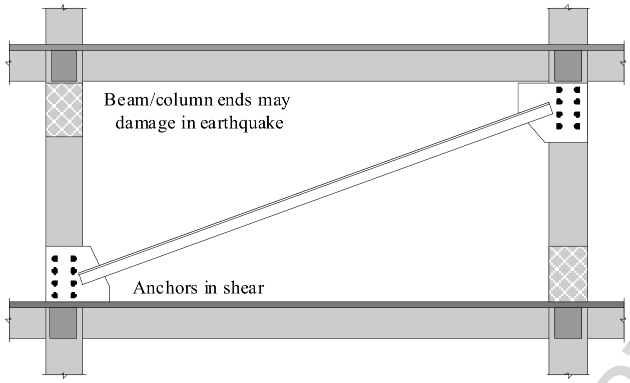


Figure 1 - Retrofit reinforced concrete frame with braces (after Badoux and Jirsa, 1990)

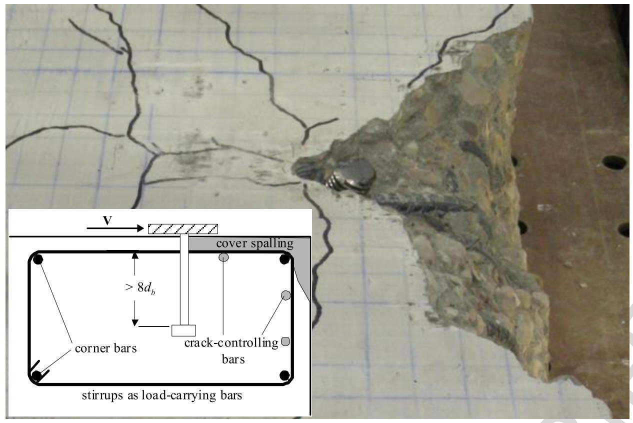


Figure 2 - Cover spalling observed in a shear test of a reinforced anchor

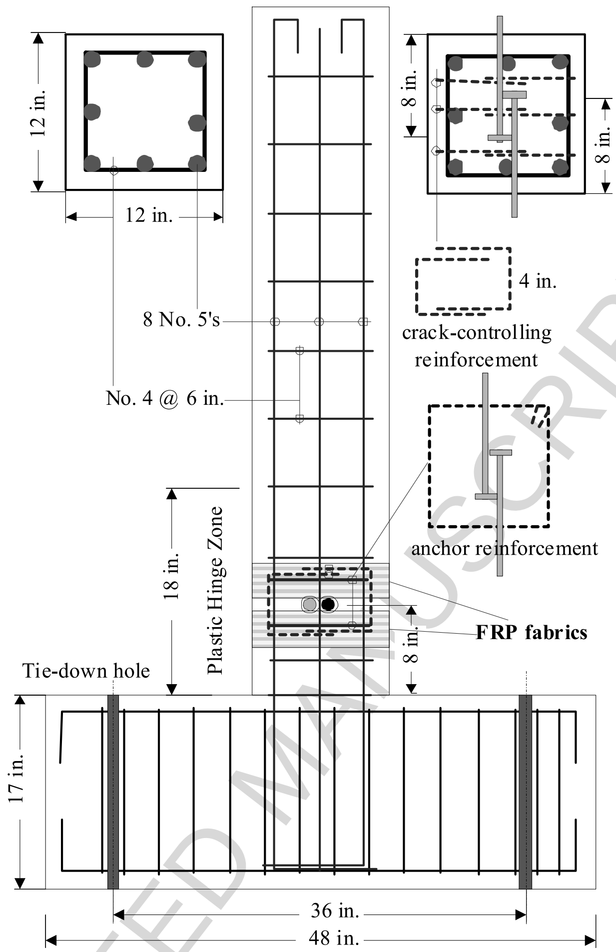


Figure 3 - Dimensions and reinforcement details of sepcimens (1 in. = 25.4 mm)

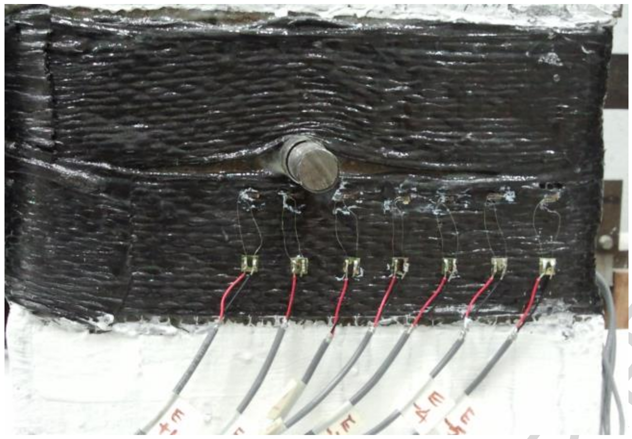

Figure 4 - Cover concrete protected by FRP fabrics and the gage locations on east face

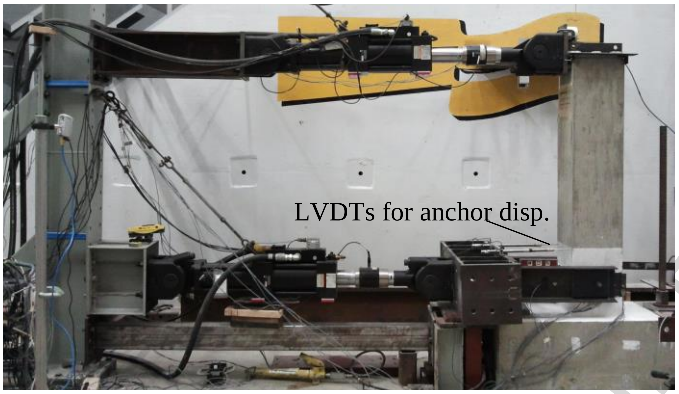

Figure 5 - Test setup for shear tests of cast-in anchors in plastic hinge zone

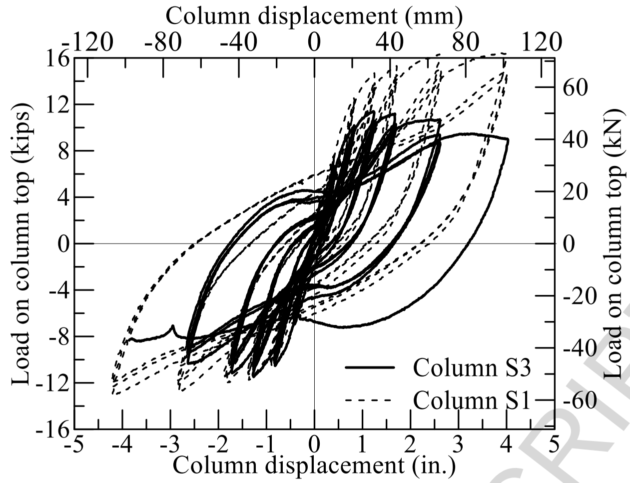


Figure 6 - Behavior of column specimens under cyclic loading

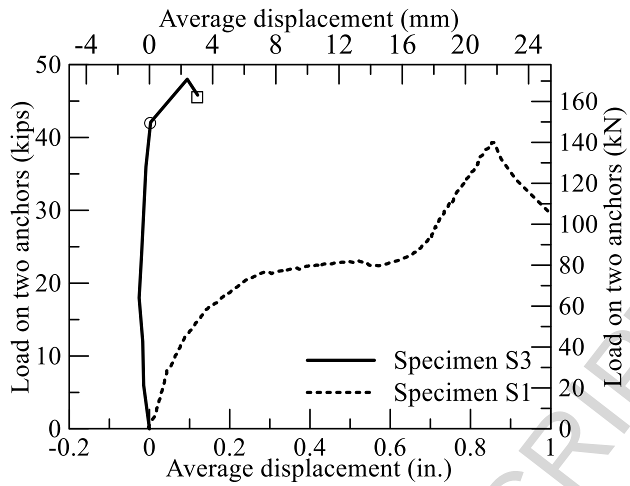


Figure 7 – Comparison of behavior of single anchors in plastic hinge zones

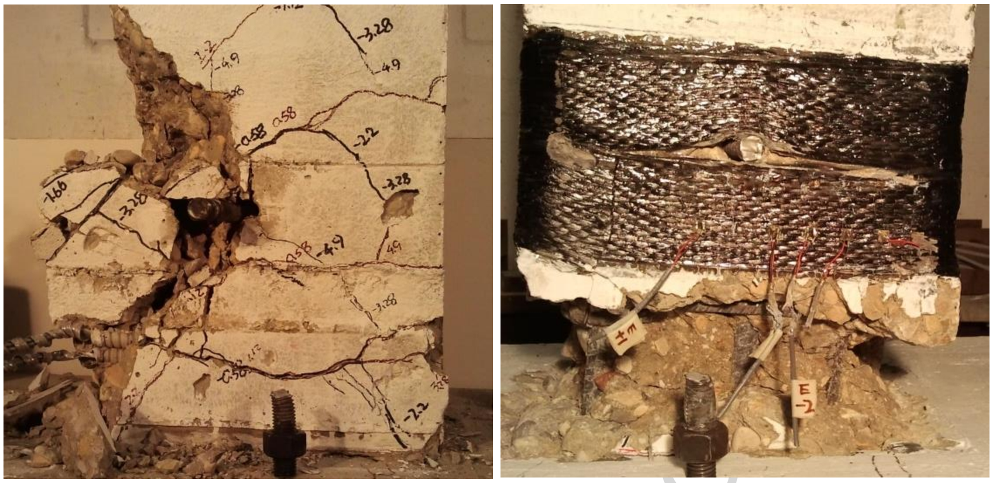

a) without cover pretection (S1) ; b) with FRP protection (S3)

Figure 8 - Concrete damage in the plastic hinge zone during the tests of anchors in shear

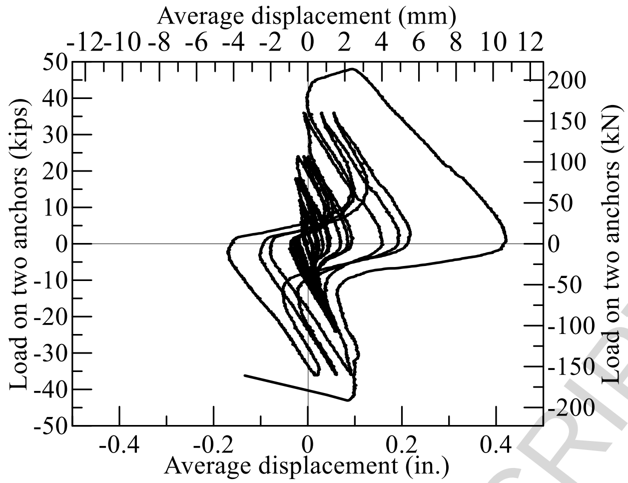


Figure 9 - Behavior of single anchors in plastic hinge zone under cyclic shear loading

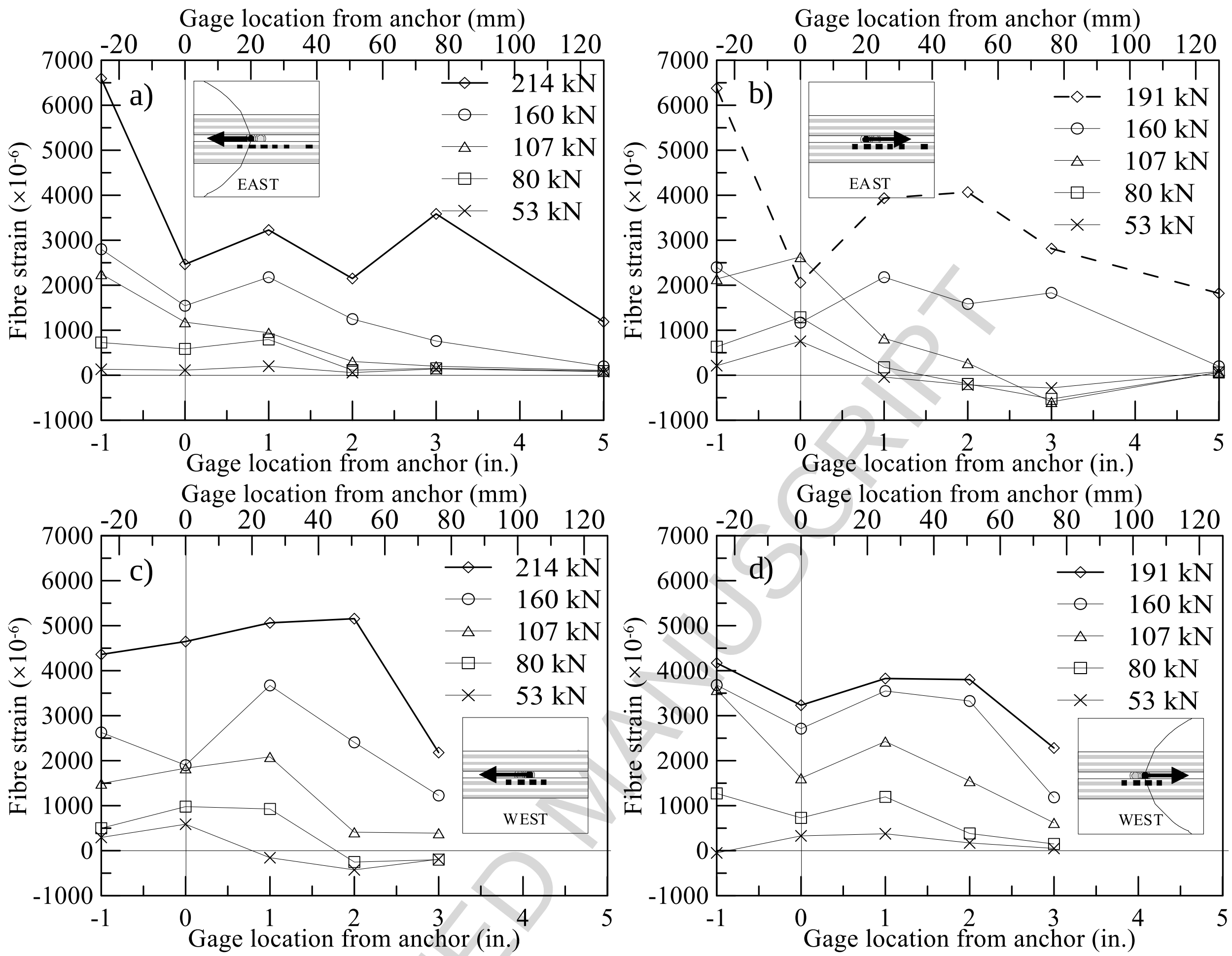


Figure 10 – Strains in the fiber bundles close to test anchors